

Supplementary information

Optimizing Citrate Combustion Synthesis of A-Site-Deficient La,Mn-Based Perovskites: Application for Catalytic CH₄ Combustion in Stoichiometric Conditions

Andrea Osti *, Lorenzo Rizzato, Jonathan Cavazzani and Antonella Glisenti *

Department of Chemical Sciences, University of Padova, Via F. Marzolo, 1, 35131 – Padova, Italy

* Correspondence: andrea.osti.1@phd.unipd.it (A.O.); antonella.glisenti@unipd.it (A.G.)

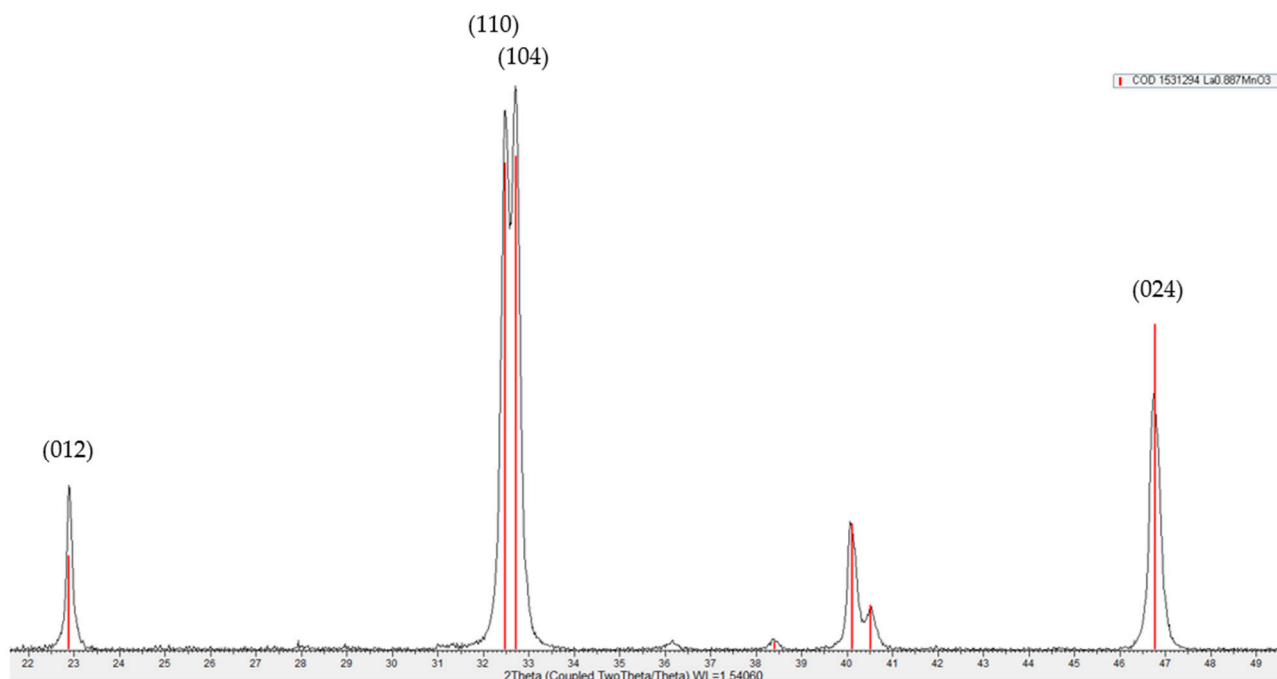


Figure S1. Extract of the XRD pattern of La_{0.8}MnO₃-NH₃-CA1.1 sample as example, showing the good matching with hexagonal La_{0.887}MnO₃ phase (COD reference 1531294). The reported (hkl) indexes are relative to the reflections fitted to obtain crystallite size by Williamson-Hall method, according to Equation S1:

$$\beta \cos \theta = \frac{K\lambda}{d} + 4\varepsilon \sin \theta \quad (\text{S1})$$

where β is the full width at half maximum of each reflection (obtained by gaussian fitting), θ is the reflection angle (radians), K a constant assumed 0.90, λ the irradiation wavelength (0.154 nm, Cu K α), d the average crystallite size (nm) and ε the crystal strain. By linear fitting of $\beta \cos \theta$ as function of $4\varepsilon \sin \theta$, the crystallite size d is obtained from the intercept and the strain ε from the slope.

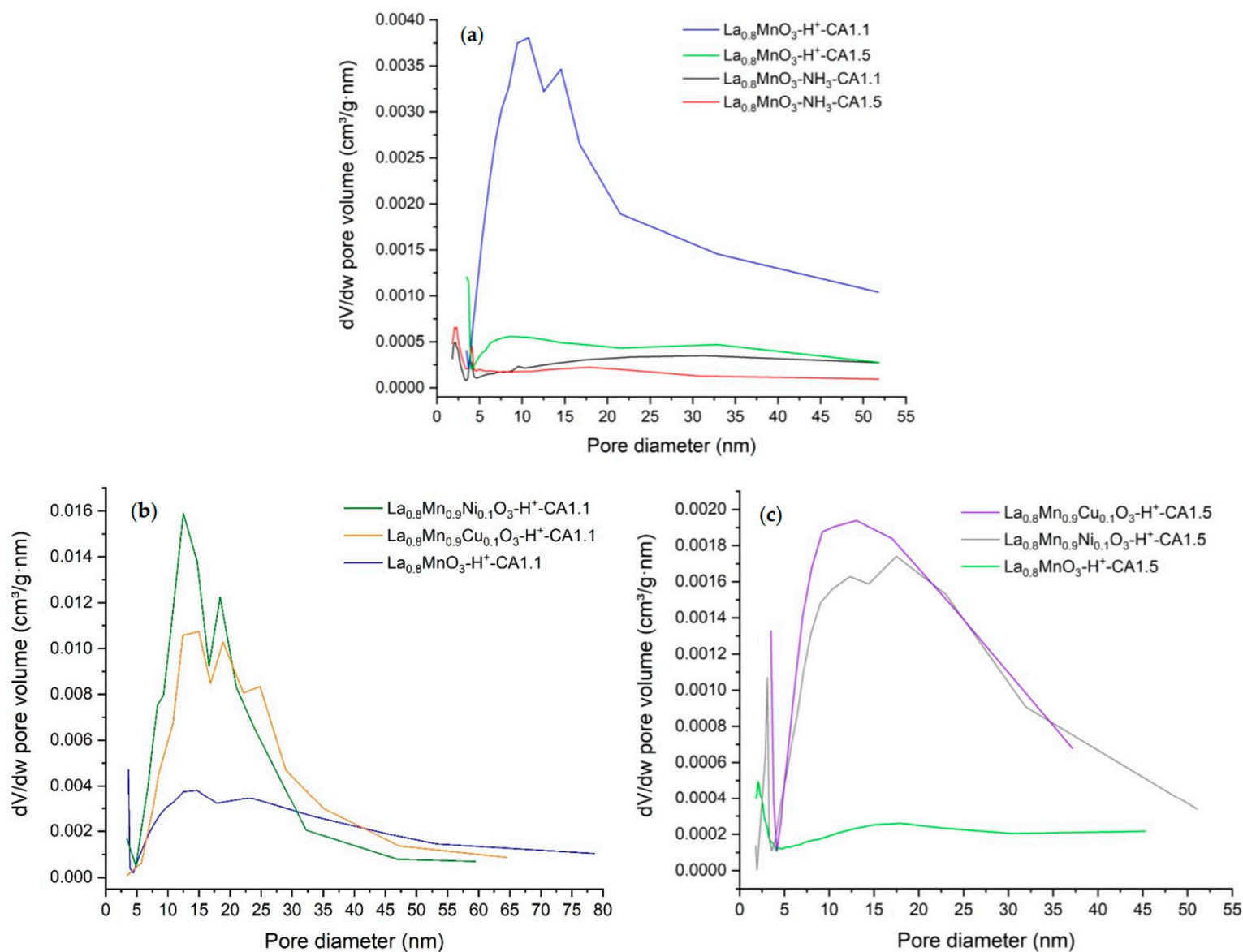


Figure S2. Pore size distribution of the prepared catalysts, according to BJH model, obtained from the desorption branch of N_2 isotherms: (a) the four $\text{La}_{0.8}\text{MnO}_3$ samples, (b) Ni- and Cu-doped samples with CA1.1, compared to $\text{La}_{0.8}\text{MnO}_3\text{-H}^+\text{-CA1.1}$, (c) Ni- and Cu-doped samples with CA1.5, compared to $\text{La}_{0.8}\text{MnO}_3\text{-H}^+\text{-CA1.5}$.

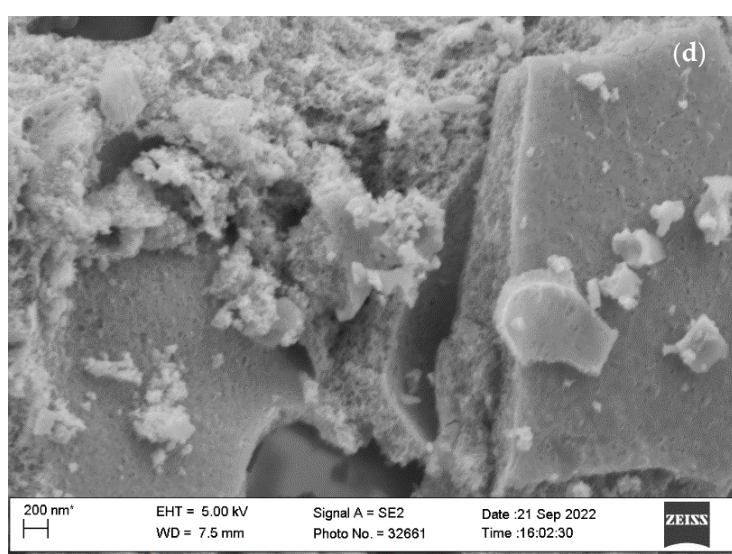
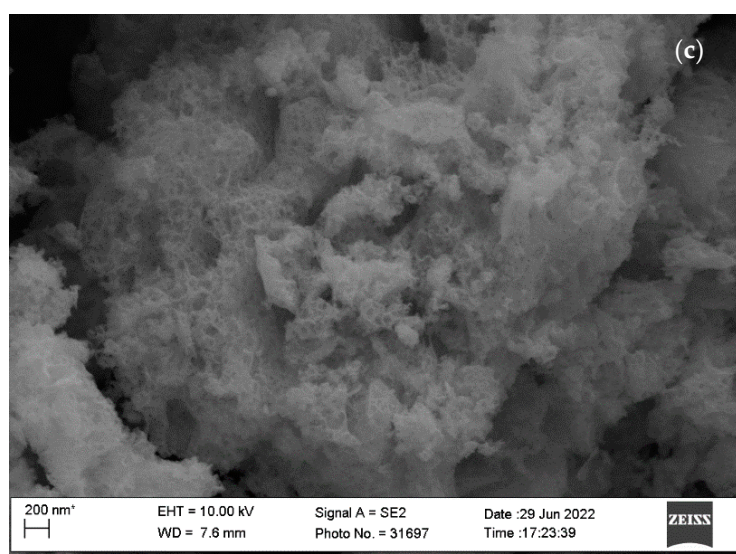
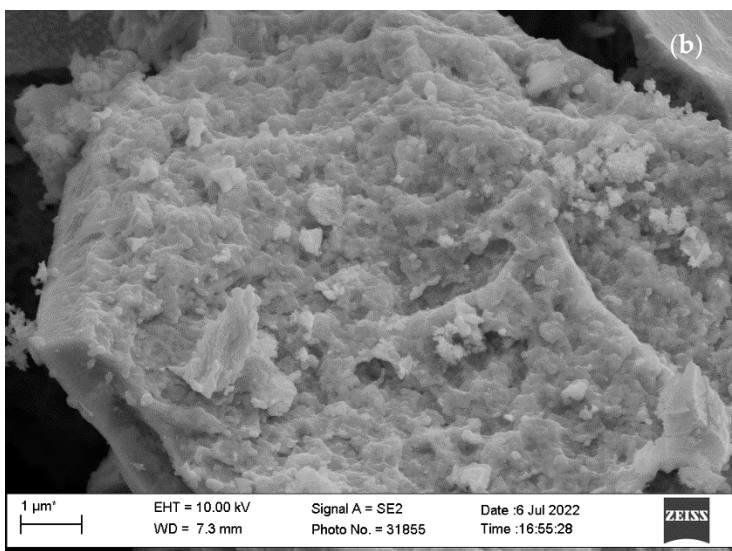
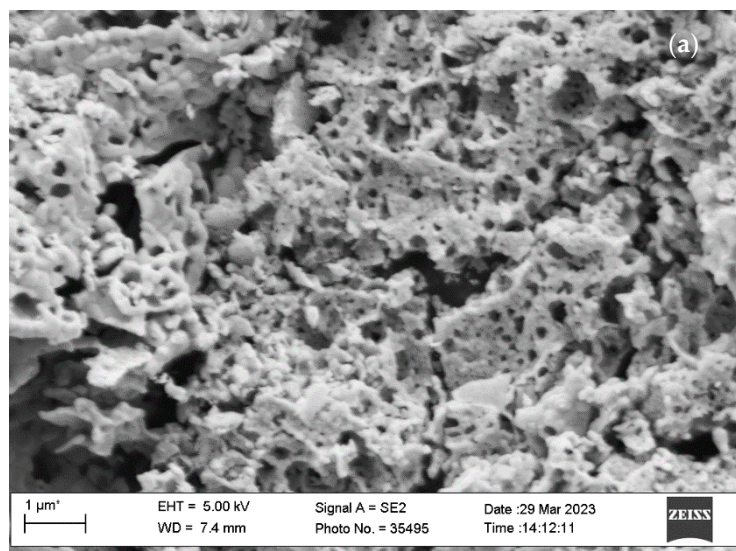


Figure S3. SEM micrographs of: (a) $\text{La}_{0.8}\text{MnO}_3\text{-NH}_3\text{-CA1.5}$; (b) $\text{La}_{0.8}\text{MnO}_3\text{-H}^+\text{-CA1.5}$; (c) $\text{La}_{0.8}\text{Mn}_{0.9}\text{Cu}_{0.1}\text{O}_3\text{-H}^+\text{-CA1.1}$; (d) $\text{La}_{0.8}\text{Mn}_{0.9}\text{Cu}_{0.1}\text{O}_3\text{-H}^+\text{-CA1.5}$. Images (a,b) are taken at 25000 \times magnification, images (c,d) at 50000 \times magnification.

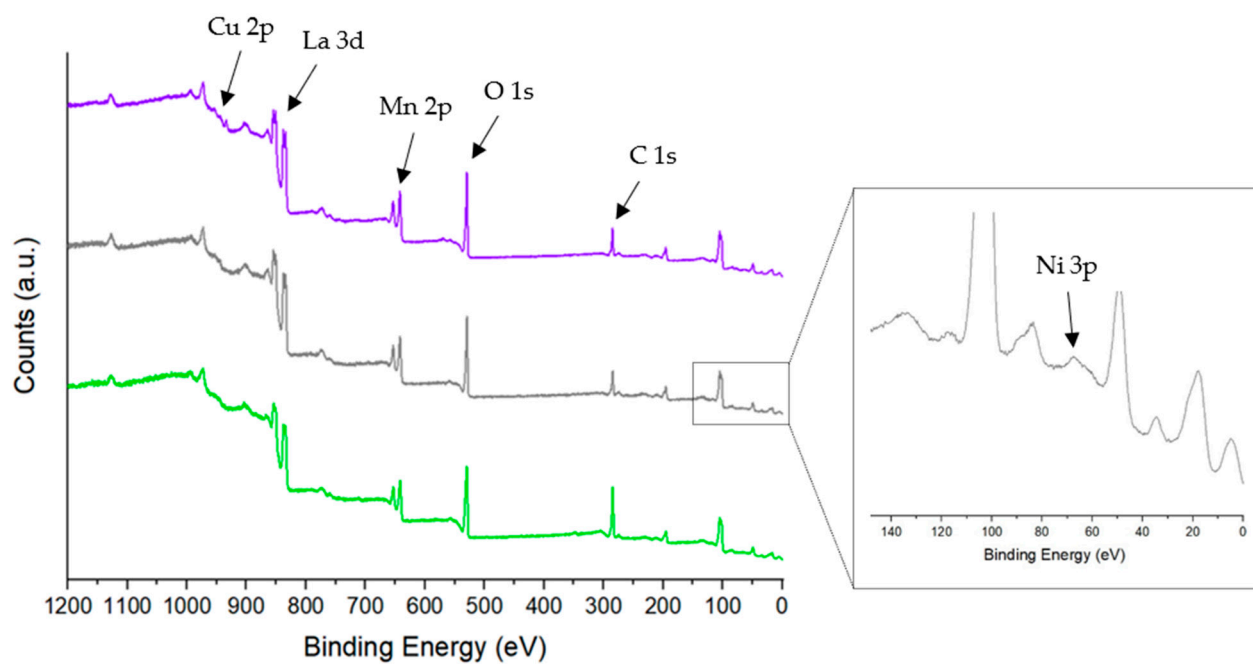


Figure S4. Representative XPS survey spectra of H^+ -CA1.5 samples and identification of the main photopeaks: $\text{La}_{0.8}\text{MnO}_3$ (green); $\text{La}_{0.8}\text{Mn}_{0.9}\text{Ni}_{0.1}\text{O}_3$ (grey), with zoom on the low binding energy region to highlight Ni3p photopeak; $\text{La}_{0.8}\text{Mn}_{0.9}\text{Cu}_{0.1}\text{O}_3$ (violet).

Table S1. EDX and XPS composition of the prepared perovskites, also considering the oxygen content (nominal amounts according to stoichiometry are reported in brackets).

Sample		O (at%)	La (at%)	Mn (at%)	Ni or Cu (at%)
La _{0.8} MnO ₃ -NH ₃ -CA1.1	EDX	64.6	17.0	18.4	/
	XPS	72.9	12.2	14.9	/
	(nominal)	(62.5)	(16.7)	(20.8)	/
La _{0.8} MnO ₃ -NH ₃ -CA1.5	EDX	72.7	12.6	14.7	/
	XPS	69.3	13.2	17.5	/
	(nominal)	(62.5)	(16.7)	(20.8)	/
La _{0.8} MnO ₃ -H ⁺ -CA1.1	EDX	66.1	17.0	16.9	/
	XPS	71.6	11.8	16.6	/
	(nominal)	(62.5)	(16.7)	(20.8)	/
La _{0.8} MnO ₃ -H ⁺ -CA1.5	EDX	65.0	16.3	18.7	/
	XPS	74.4	10.7	14.9	/
	(nominal)	(62.5)	(16.7)	(20.8)	/
La _{0.8} Mn _{0.9} Ni _{0.1} O ₃ -H ⁺ -CA1.1	EDX	67.0	16.1	15.3	1.6
	XPS	66.5	12.7	20.1	0.7
	(nominal)	(62.5)	(16.7)	(18.8)	(2.1)
La _{0.8} Mn _{0.9} Ni _{0.1} O ₃ -H ⁺ -CA1.5	EDX	63.3	17.7	16.8	2.2
	XPS	66.5	13.3	18.8	1.4
	(nominal)	(62.5)	(16.7)	(18.8)	(2.1)
La _{0.8} Mn _{0.9} Cu _{0.1} O ₃ -H ⁺ -CA1.1	EDX	67.7	15.5	15.6	1.2
	XPS	63.5	13.6	18.8	4.1
	(nominal)	(62.5)	(16.7)	(18.8)	(2.1)
La _{0.8} Mn _{0.9} Cu _{0.1} O ₃ -H ⁺ -CA1.5	EDX	64.9	16.9	16.0	2.2
	XPS	65.5	12.3	18.5	3.7
	(nominal)	(62.5)	(16.7)	(18.7)	(2.1)